Available at
www.ElsevierMathematics.com
POWERED BY SCIENCE DIRECT®

ELSEVIER Journal of Computational and Applied Mathematics 164–165 (2004) 629–641

JOURNAL OF COMPUTATIONAL AND APPLIED MATHEMATICS

www.elsevier.com/locate/cam

Simultaneous solution approaches for large optimization problems

Volker Schulz

Department of Mathematics, University of Trier, FB IV, Trier D-54286, Germany

Received 20 August 2002; received in revised form 11 July 2003

Abstract

In this paper, efficient simultaneous strategies are presented for the optimization of practical problems involving PDE-models. In particular, reduced sequential quadratic programming methods for problems with only few influence variables and simultaneous quadratic programming iterations are discussed. As a result we obtain algorithms whose overall computational complexity is reduced considerably in comparison to a black-box approach.

Keywords: Partially reduced SQP methods; Iterative QP solvers; Bingham flow; Topology design

1. Introduction and motivational problem

The industrial acceptance of mathematical optimization methods not only depends on the computational effort to achieve optimal solutions, but also on their implementational ease. In particular in applications involving PDE-models, many practitioners still use the so-called black-box approach. Here, simultaneous algorithmic approaches for real world problems are presented which possess a low computational complexity but are nevertheless of implementational simplicity (at least in the first part of the paper). Two applications are discussed: parameter identification of Bingham flow and topology design in electromagnetics.

The first practical problem to be considered is the material characterization of non-Newtonian fluids on the basis of pressure measurements. The problem formulation is the outcome of a joint project with the company Braun Inc. in Friedrichshafen, Germany, in collaboration with the research group of Gabriel Wittum, IWR, University of Heidelberg, Germany.

E-mail address: volker.schulz@uni-trier.de (V. Schulz).

0377-0427/$ - see front matter
doi:10.1016/j.cam.2003.09.011

Braun Inc. produces forming dies for extrusion devices of pastes used in the production of ceramic wafers for catalysts in automotives, power stations and medicine, as well as bricks and tiles and similar things. There are high demands on material properties of ceramic bodies such as fracture resistance, shape stability, porosity, heat conductivity, etc. The production of forming dies is very expensive, therefore, numerical simulation methods which reduce the necessary number of hardware prototypes have a natural economic appeal. Typically, the shaping of ceramic bodies is performed by augers of extruders, where the actual shaping takes place in the pressing tool composed of a die connected to a pressure head. The ceramic fluid pressed through the die is considered as a viscoplastic fluid with wall slip and is characterized by a Bingham model involving four model parameters. The stationary flow considered here is described by the following PDE for velocity $\mathbf{u}$ and pressure p:

$$\begin{aligned} &\operatorname{div}\mathbf{u} = 0, \\ &-\operatorname{div}(2\mu(\mathbf{D})\cdot\mathbf{D}) + \nabla p = 0. \end{aligned} \tag{1}$$

Here, the nonlinear viscosity μ depends on the strain tensor

$$\mathbf{D} = \tfrac{1}{2}(\nabla\mathbf{u} + (\nabla\mathbf{u})^{\top})$$

in the way

$$\mu(\mathbf{D}) = \eta_{\mathrm{B}} + \tau_{\mathrm{F}}(2\mathbb{I}_{\mathbf{D}})^{-1/2}, \tag{2}$$

where $\mathbb{I}_{\mathbf{D}}$ is the second invariant of $\mathbf{D}$, $\mathbb{I}_{\mathbf{D}} = \frac{1}{2}(\operatorname{trace}\mathbf{D}^2 - (\operatorname{trace}\mathbf{D})^2)$.

These Bingham flow equations involve two material parameters, the Bingham viscosity η_{B} and the yield stress τ_{F}. The nonlinear viscosity term (2) leads to severe numerical problems in regions of small velocity variations. There, one should ideally switch to a flow with constant velocity, which can be done, e.g., in the form of variational inequalities. Here we use an alternative approach, where we regularize Eq. (1). This means that we introduce a small parameter δ in the generalized viscosity function μ, so that

$$\mu(\mathbf{D}) = \eta_{\mathrm{B}} + \tau_{\mathrm{F}}(\delta + 2\mathbb{I}_{\mathbf{D}})^{-1/2}. \tag{3}$$

Thus, we get an approximation of system (1) at which μ is bounded. The solution of the regularized system deviates from the unregularized Bingham solution. An exploration of the regularization error in a model problem is carried out in [8], where, it is shown that this error tends to zero like $\mathrm{O}(\sqrt{\delta})$.

In addition to these equations, the model of the ceramic pastes requires special boundary conditions. The reason is a phenomenon called wall sliding. Microscopically, we have a two-phase flow on the boundary yielding a lubrication effect. Macroscopically, this is described by sliding, resulting in a Navier-type boundary condition that, in 2D, has the form

$$\begin{aligned} &\mathbf{n}^{\mathrm{T}}\mathbf{T}\mathbf{t} = k\mathbf{u}^{\mathrm{T}}\mathbf{t} + \tau_{\mathrm{G}}, \\ &\mathbf{u}^{\mathrm{T}}\mathbf{n} = 0, \end{aligned} \tag{4}$$

where $\mathbf{t}$ and $\mathbf{n}$ are the unit normal and unit tangent vectors to the boundary, respectively. Here we assume that the tangential stress and the tangential velocity are codirected on the boundary. These conditions include two additional scalar parameters: a wall sliding factor k and a sliding limit τ_{G}.

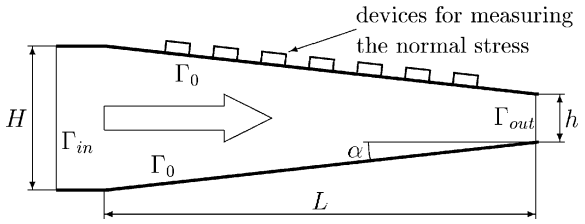

Fig. 1. Scheme of the measurement device.

Thus, for the mathematical description of the flows of the ceramic pastes we have the system of PDEs (1) with the boundary conditions (4) on walls. (Besides inflow and outflow boundary conditions can be imposed on some parts of the boundary.) The whole model involves four parameters: η_B, τ_F, k, and τ_G. The aim of the parameter estimation procedure described here is to find these values by using experimental data obtained by the device described in the next section. The nonlinearity of the PDE system together with its boundary conditions poses a considerable challenge to the numerical treatment of the resulting parameter identification problem. Additionally it is necessary to note as well that the pressure p is defined by this system only up to a constant. Methods for the discretization of this system and the numerical solution of the resulting nonlinear discrete equations are considered in detail in [7,8].

The parameters are estimated by using data obtained from a device whose scheme is shown in Fig. 1. This is a conical channel with rigid walls. The paste is pressed through this channel at a constant velocity in the direction of the large arrow. During this process, we measure the normal stress at seven fixed points on the upper wall (further referred to as *measurement points*). The values of the normal stress, as well as the inflow velocity of the paste, are then used for the parameter identification.

In order to model the flow of the paste inside the device we consider the interior (the polygon) as a region Ω on which we impose the PDE system (1) with the generalized viscosity function. On the part $\Gamma_0 \subset \partial\Omega$ of the boundary corresponding to the rigid walls we assume boundary conditions (4). On the inflow boundary Γ_{in} we impose Dirichlet boundary conditions for the velocity specifying the constant inflow velocity v_0 along the whole segment. On the outflow boundary Γ_{out} we impose zero vertical velocity as boundary condition and require $\int_{\Gamma_{\text{out}}} p\,\mathrm{d}s = \text{const}$. For every set $q = (\eta_B, \tau_F, k, \tau_G)^T$ of four parameters this system defines the velocity field $\mathbf{u}$ and the pressure field p. Besides, we write all the partial differential equations comprising system (1) and the boundary conditions in the form

$$\mathbf{c}(\mathbf{u}, p, q) = 0. \tag{5}$$

Denote the measurement points by $P_1, P_2, \ldots, P_K$ (in our case $K = 7$), in flow direction. For every P_i we have a measured value $\hat{\pi}_i$ of the normal stress. Simultaneously, for every given set q of the parameters we can get the fields $\mathbf{u}$ and p from Eq. (5) and compute the normal stress $\pi_P(\mathbf{u}, p, q)$ at every point $P \in \Gamma_0$:

$$\pi_P(\mathbf{u}, p, q) = \mathbf{n}_P^T \mathbf{T}_P(\mathbf{u}, p, q)\,\mathbf{n}_P,$$

where $\mathbf{n}_P$ and $\mathbf{T}_P(\mathbf{u}, p, q)$, respectively, are the unit normal vector to the boundary and the stress tensor at the point P. The "correct" parameters are then determined as the solution of the nonlinear

constrained optimization problem

$$f(\mathbf{u}, p, q) = \sum_{i=2}^{K} \frac{1}{\sigma_i^2} ((\pi_{P_i}(\mathbf{u}, p, q) - \pi_{P_1}(\mathbf{u}, p, q)) - (\hat{\pi}_i - \hat{\pi}_1))^2 \to \min,$$

$$\text{s. t. } \mathbf{c}(\mathbf{u}, p, q) = 0, \tag{6}$$

where $\sigma_i = 0.08(\hat{\pi}_i + \hat{\pi}_1)$ are the standard deviations for the difference evaluations, if all measurements are assumed to be independently normally distributed with expectation $\hat{\pi}_i$ and standard deviation $0.08\hat{\pi}_i$. Although the model defines the normal stress only up to a constant, the differences of the stresses are defined exactly and should approximate the differences of the measured normal stresses. The numerical solution is carried out in a direct approach, i.e., by discretization of the model and the objective functional. This leads to a finite dimensional nonlinearly constrained optimization problem of a very large size that requires the application of structure exploiting methods in order to reduce the computation time.

Further details of the problem formulation and the discretization can be found in [14].

2. Black-box versus reduced SQP approaches

The least-squares optimization problem (6) involves the solution of a discretized PDE as an underlying problem. The solution of the discretized PDE typically involves an iterative technique by its own. Therefore, an obvious and often used approach for the solution of the overall optimization problem is the use of a nested loop approach, where in an outer iteration cycle an optimization algorithm iterates over the optimization influence variable and an inner loop over the PDE model variables guarantees feasibility of all intermediate steps. This is also called "black-box approach" since the inner PDE-loop is treated as a black-box, producing solution variables for the PDE for a given problem formulation, where during the optimization process one does not care what kind of inner processes this black-box involves.

There are cases in practical applications where feasibility at all costs is an issue, but they are rare. In most practical problems, fasibility is only required for the solution of the optimization problem. This fact can be exploited in such a way that one replaces the inner black-box iteration process by, e.g., just one iteration of that process. If we consider a Newton-type method for the inner loop with an iterative linear solver, then one might conceive using just one Newton step instead of the whole Newton iteration or even just one step of the linear solver within the Newton method.

The latter type of optimization strategies are called simultaneous strategies. All those simultaneous strategies must be justified by convergence considerations. To be more specific, we consider the following abstract optimization problem formulation:

$$\begin{aligned} \min_{x,q} \quad & f(x,q), \quad f : \mathbb{R}^{n_x+n_q} \to \mathbb{R}, \\ \text{s.t.} \quad & c(x,q) = 0, \quad c : \mathbb{R}^{n_x+n_q} \to \mathbb{R}^{n_x}, \ C_x := \partial c/\partial x \text{ nonsingular}, \\ & g(q) \geqslant 0, \quad g : \mathbb{R}^{n_q} \to \mathbb{R}^{n_g}, \end{aligned} \tag{7}$$

where $x \in \mathbb{R}^{n_x}, q \in \mathbb{R}^{n_q}$. The cost functional f denotes the output least squares objective here. The equality constraint c summarizes the discretized flow equations as discussed in the previous section

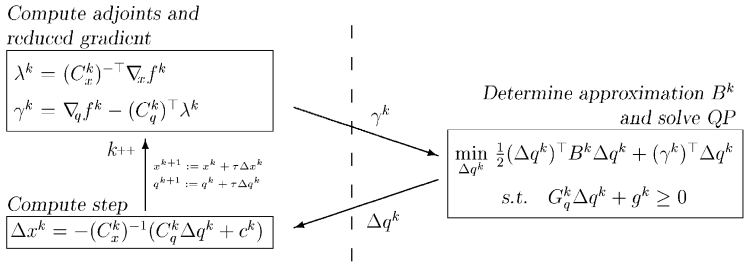

Fig. 2. Sketch of a PRSQP method.

for the flow state variables x and the model parameters q. The inequality constraint collects typical range constraints for the parameters which are always tacidly stated. We assume sufficiently high differentiability of all functions involved. The condition C_x nonsingular reflects the natural assumption that the flow equations can always be solved. From that assumption we can conclude the existence of a mapping

$$x : q \mapsto x(q) \quad \text{such that } c(x(q), q) = 0.$$

Thus, we can restate the optimization problem as

$$\begin{aligned} &\min_q \quad f(x(q), q), \\ &\text{s.t.} \quad g(q) \geqslant 0. \end{aligned} \tag{8}$$

The application of a sequential quadratic programming (SQP) technique to that problem formulation, where for each parameter value q one has to provide an inner solution procedure in order to obtain a consistent value $x(q)$ is an example of a method within the black-box approach. If we break up the corresponding nested loop by performing just one single Newton iteration in the inner loop, we obtain the following algorithm:

A conceptual PRSQP method is sketched in Fig. 2.

Indices k mean evaluation at the kth iterate. One observes that although the algorithm iterates simultaneously over both types of variables—with state increments Δx^k and parameter increments Δq^k—it can be decoupled from an implementation point of view into a PDE and adjoint PDE part and an optimization part. This kind of modularity is highly appreciated in real applications. The matrices B^k are approximations of the Hessian of the Lagrangian

$$\hat{\mathscr{L}}(q) := f(x(q), q) - \mu^\top g(q).$$

It can be shown that

$$\partial^2 \hat{\mathscr{L}}(q)/\partial q^2 = T^\top \partial^2 \mathscr{L}(x, q)/\partial(x, q)^2 T,$$

where

$$\mathscr{L}(x, q) := f(x, q) - \lambda^\top c(x, q) - \mu^\top g(q),$$

denotes the Lagrangian of the original problem and

$$T := \begin{bmatrix} -C_x^{-1} C_q \\ I \end{bmatrix} \quad \text{a basis of the kernel of} \quad C = \begin{bmatrix} C_x & C_q \end{bmatrix}.$$

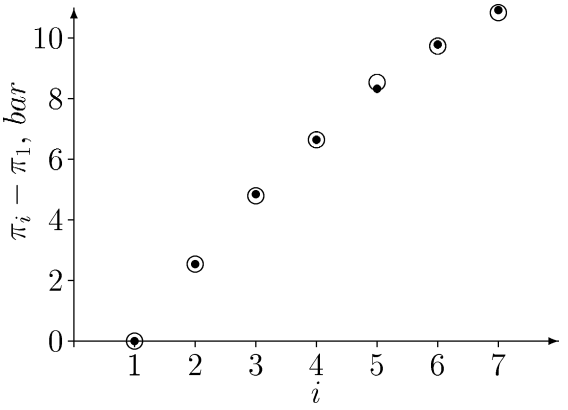

Fig. 3. The differences of the normal stresses. Empty circles denote the relative measured stresses ($\hat{\pi}_i - \hat{\pi}_1$), the black circles show the stresses $\pi_{h,i}(\mathbf{x}, q) - \pi_{h,1}(\mathbf{x}, q)$ computed for the final guess of the optimization procedure.

In the context of SQP methods the latter Hessian is called the reduced Hessian and also the method discussed above is called a reduced SQP method. The reduced Hessian is not built up exactly but it is rather approximated typically by update formulas of Broyden type. Since the problem is not reduce up to the kernel of all active constraints, we call this method a partially reduced SQP method if we want to emphasize this fact.

Reduced SQP methods are specific variants of SQP methods for overall constrained optimization problems, which gives rise to the underlying convergence theory (cf. [11]). In dealing with applications of the type discussed in Section 2, one even has to cope with inexact linear solvers within the reduced SQP approach. Details to that problem are discussed in [14]. The resulting algorithm yields the results depicted in Fig. 3.

The computations have been performed on a SGI Indigo2 with R4400 processor and took 767 s. As a comparison, a single computation of the velocity and pressure field took 318 s on the same machine, which means that the simultaneous approach enabled us in this example to solve the whole optimization problem in only approximately double the time necessary for the solution of the forward problem. Similar advantageous computing times are also reported for turbine blade optimization problems in [4].

Remark. In contrast to that, a black-box SQP approach needs even for a completely linear problem at least four SQP-iterations for convergence, where each iteration costs approximately twice the effort as one flow solution because the adjoint solver is iterative and approximately as expensive as the forward solver. In total, that means at least a factor of eight compared to a forward flow solution.

3. Simultaneous QP solution

The simultaneous optimization strategy developed in the previous section is most advantageous when the number of influence variables is comparatively low—because of the use of update formulas. Also in different settings, however, simultaneous strategies can be developed on the basis of SQP

methods. Here, we present a practical example where the quadratic subproblems within a SQP method are solved by a simultaneous iterative solver. The problem considered is the topology optimization of electromagnetic media described by Maxwell's equations. This is a joint work together with R.H.W. Hoppe and S. Petrova from the University of Augsburg.

We are looking for an optimal distribution of conductivity in a fixed geometrical configuration. In the stationary case, one obtains problem formulations in electro- and magneto-statics, which are similar to elasto–mechanical problems. The mathematical models lead to elliptic boundary value problems corresponding to a minimization of energy dissipation given by the Joule–Lenz law. We suppose that our domain is occupied by an isotropic conductor with a finite conductivity. In order to simplify the presentation, we consider the stationary case, i.e., constant currents are available in the conductor.

We consider electromagnetic fields in the low-frequency regime which can be described by the quasi-stationary limit of Maxwell's equations also known as the eddy currents equations

$$\frac{\partial \mathbf{B}}{\partial t} + \operatorname{curl} \mathbf{E} = \mathbf{0}, \quad \operatorname{div} \mathbf{B} = 0, \quad \operatorname{curl} \mathbf{H} = \mathbf{J}, \tag{9}$$

$$\mathbf{B} = \mu \mathbf{H}, \quad \mathbf{J} = \sigma \mathbf{E}. \tag{10}$$

Here, $\mathbf{E}$ and $\mathbf{H}$ stand for the electric and magnetic fields, respectively, $\mathbf{B}$ and $\mathbf{J}$ denote the magnetic induction and the current density, and μ and σ refer to the magnetic permeability and the electric conductivity, respectively (for a justification of the eddy currents equations see, e.g. [1]).

In the 2D case, assuming the current density to be given by

$$\mathbf{J} = (J_1(x_1, x_2, t), J_2(x_1, x_2, t), 0),$$

the electric and magnetic fields take the form

$$\mathbf{E} = (E_1(x_1, x_2, t), E_2(x_1, x_2, t), 0), \quad \mathbf{H} = (0, 0, H(x_1, x_2, t)).$$

We use a potential formulation by introducing a scalar electric potential φ and a magnetic vector potential $\mathbf{A}$ according to

$$\mathbf{E} = -\,\mathbf{grad}\, \varphi - \frac{\partial \mathbf{A}}{\partial t}, \quad B = \operatorname{curl} \mathbf{A}$$

where curl is the 2D scalar operator $\operatorname{curl}(A_1, A_2) = \partial A_1/(\partial x_2) - \partial A_2/(\partial x_1)$ (cf. [3]). Then, (9)–(10) give rise to the following coupled system of PDEs for the electromagnetic potentials φ and $\mathbf{A}$

$$\operatorname{div}(\sigma\, \mathbf{grad}\, \varphi) = 0 \text{ in } \Omega, \tag{11}$$

$$\sigma \mathbf{n} \cdot \mathbf{grad}\, \varphi = \begin{cases} I_v & \text{given data on } \Gamma_v \subset \partial\Omega, \\ 0 & \text{else}, \end{cases} \tag{12}$$

$$\sigma \frac{\partial \mathbf{A}}{\partial t} + \operatorname{curl} \mu^{-1} \operatorname{curl} \mathbf{A} = \begin{cases} -\sigma\, \mathbf{grad}\, \varphi & \text{in } \Omega, \\ 0 & \text{in } \mathbb{R}^2 \setminus \bar{\Omega}, \end{cases} \tag{13}$$

the latter one with appropriate initial and boundary conditions.

Note that in (12) we refer to I_v as the fluxes associated with the contacts $\Gamma_v \subset \partial\Omega, 1 \leqslant v \leqslant N_c$, satisfying the compatibility conditions $\sum_{v=1}^{N_c} I_v = 0$.

The electric energy dissipation given by the Joule–Lenz law reads as follows:

$$f(\varphi, \sigma, \mathbf{A}) := \int_\Omega \mathbf{J} \cdot \mathbf{E} \, \mathrm{d}x. \tag{14}$$

In particular, in the stationary regime this reduces to

$$f(\varphi, \sigma) = -\int_\Omega \mathbf{J} \cdot \mathbf{grad}\, \varphi \, \mathrm{d}x = -\int_\Omega \mathrm{div}(\varphi \mathbf{J}) \, \mathrm{d}x. \tag{15}$$

The last equality in (15) follows from $\mathrm{div}(\varphi\mathbf{J}) = \mathbf{J} \cdot \mathbf{grad}\, \varphi + \varphi \,\mathrm{div}\, \mathbf{J}$, taking into account that $\mathrm{div}\, \mathbf{J} = 0$ in view of (9).

Using Gauss' theorem and the Neumann boundary conditions from (12) we get

$$f(\varphi, \sigma) = -\int_{\partial\Omega} \mathbf{n} \cdot \mathbf{J} \, \mathrm{d}s \, \varphi = \sum_{v=1}^{N_c} \int_{\Gamma_v} I_v \varphi \, \mathrm{d}s. \tag{16}$$

We solve the optimization problem for the energy dissipation given by (16).

Find

$$\min_{\varphi,\sigma} \; f(\varphi, \sigma) = \min_{\varphi,\sigma} \sum_v \int_{\Gamma_v} I_v \varphi \, \mathrm{d}s, \tag{17}$$

subject to the following constraints:

$$\begin{aligned} &\varphi \text{ satisfies (11)–(12)}, \\ &\int_\Omega \sigma \, \mathrm{d}x = C \quad \text{(mass constraint)}, \\ &\sigma_{\min} \leqslant \sigma \leqslant \sigma_{\max} \quad \text{(conductivity box constraint)}. \end{aligned} \tag{18}$$

Here, $\sigma_{\min}$ and $\sigma_{\max}$ are a priori given positive limits for the conductivity and C is a fixed given value. In general formulations of nonlinear programming problems, the objective function f and the inequality constraints are supposed to be twice continuously differentiable. In our case this requirement is obviously satisfied.

After a finite element discretization of the domain with a discretization parameter h we get the following finite dimensional nonlinear programming problem, where we identify the vector x with the discretized state variable ϕ and the free variable vector q with the discretized conductivity σ.

$$\min_{x,q} \quad f(x, q), \tag{19}$$

s.t.

$$\begin{aligned} &A(q)x - \mathbf{b} = 0, \quad q - \sigma_{\min}\mathbf{e} \geqslant 0, \\ &g(q) - \mathrm{C} = 0, \quad \sigma_{\max}\mathbf{e} - q \geqslant 0, \end{aligned} \tag{20}$$

where $\mathbf{e} = (1, \ldots, 1)^{\mathrm{T}}$. Here, A is the finite element stiffness matrix and $\mathbf{b}$ is the discrete load vector. Note that the objective function (19) is just a more abstract reformulation of (17). Since the values I_v in (17) are given data, the objective function is linear in $x = \phi$ and does not depend on $q = \sigma$ at all.

The *Lagrangian function* associated with problem (19)–(20) is

$$\begin{aligned}\mathscr{L}(x,q,\lambda,\eta,\mathbf{z},\mathbf{w}) := & f(x,q)\\ & + \lambda^{\mathrm{T}}(A(q)x-\mathbf{b}) + \eta\,(g(q)-\mathrm{C})\\ & - \mathbf{z}^{\mathrm{T}}(q-\sigma_{\min}\mathbf{e}) - \mathbf{w}^{\mathrm{T}}(\sigma_{\max}\mathbf{e}-q).\end{aligned} \tag{21}$$

Here, λ, η and $\mathbf{z}\geqslant 0$, $\mathbf{w}\geqslant 0$ are the Lagrange multipliers for the equality and inequality constraints in (20), respectively. The necessary first-order Karush–Kuhn–Tucker (KKT) optimality conditions read as follows:

$$\begin{aligned}&\nabla_x\mathscr{L} = \nabla_x f + A(q)^{\mathrm{T}}\lambda = 0,\\ &\nabla_q\mathscr{L} = \partial_q(\lambda^{\mathrm{T}}A(q)x) + \eta\nabla g(q) - \mathbf{z} + \mathbf{w} = 0,\\ &\nabla_\lambda\mathscr{L} = A(q)x - \mathbf{b} = 0,\\ &\nabla_\eta\mathscr{L} = g(q) - C = 0,\\ &D_1\mathbf{z} = 0 \quad \text{and} \quad D_2\mathbf{w} = 0, \quad \mathbf{z}\geqslant 0,\ \mathbf{w}\geqslant 0,\end{aligned} \tag{22}$$

where $D_1 = \mathrm{diag}(\sigma_i - \sigma_{\min})$ and $D_2 = \mathrm{diag}(\sigma_{\max} - \sigma_i)$ denote diagonal matrices in the complementarity conditions.

The *Hessian* of the Lagrangian with respect to (x,q) is denoted by

$$H = H(x,q,\lambda) = \begin{pmatrix} 0 & \mathscr{L}_{xq}\\ \mathscr{L}_{qx} & \mathscr{L}_{qq}\end{pmatrix}, \tag{23}$$

where

$$\begin{aligned}&\mathscr{L}_{qx} = \mathscr{L}_{xq}^{\mathrm{T}} = \partial_q(\lambda^{\mathrm{T}}A(q)),\\ &\mathscr{L}_{qq} = \partial_{qq}^2(\lambda^{\mathrm{T}}A(q)x).\end{aligned}$$

Our purpose is to find an isolated (locally unique) local minimum of the problem (19)–(20). We apply a primal–dual interior point approach involving a barrier function.

The logarithmic barrier function associated with the optimization problem (19)–(20) consists of solving a sequence of minimization subproblems of the form

$$\begin{aligned}&\min_{x,q}\beta(x,q,p),\\ &\beta(x,q,p) := f(x,q) - p(\log(q-\sigma_{\min}\mathbf{e}) + \log(\sigma_{\max}\mathbf{e}-q)),\end{aligned} \tag{24}$$

subject to equality constraints

$$A(q)\,x - \mathbf{b} = 0 \quad \text{and} \quad g(q) - C = 0, \tag{25}$$

where $\beta(x,q,p)$ is the *barrier function* and $p>0$ is the *barrier parameter*. We suppose here that $q > \sigma_{\min}\mathbf{e}$ and $\sigma_{\max}\mathbf{e} > q$, so that the logarithmic terms serve as a barrier. This method is obviously an interior–point method in the sense that it keeps iterates strictly feasible with respect to the inequality

constraints. The subproblems (24)–(25) are solved for decreasing values of p and have the following Lagrangian:

$$\mathscr{L}_p(x,q,\lambda,\eta) := \beta(x,q,p) + \lambda^{\mathrm{T}}(A(q)x - \mathbf{b}) + \eta\,(g(q) - C).$$

The first-order KKT conditions for the logarithmic barrier optimization subproblems result in

$$\begin{aligned}
&\nabla_x \mathscr{L}_p = \nabla_x f + A(q)^{\mathrm{T}}\lambda = 0,\\
&\nabla_q \mathscr{L}_p = \partial_q(\lambda^{\mathrm{T}}A(q)x) + \eta\nabla \mathrm{g}(q) - p\,D_1^{-1}\mathbf{e} + p\,D_2^{-1}\mathbf{e} = 0,\\
&\nabla_\lambda \mathscr{L}_p = A(q)x - \mathbf{b} = 0,\\
&\nabla_\eta \mathscr{L}_p = g(q) - C = 0.
\end{aligned} \tag{26}$$

A comparison of the second rows in (22) and (26) reveals that the terms $p\,D_1^{-1}\mathbf{e}$ and $p\,D_2^{-1}\mathbf{e}$ may serve as Lagrange multipliers $\mathbf{z}$ and $\mathbf{w}$ for the inequality constraints. The interior–point method is now characterized by substituting the last two complementarity conditions in (22) by the *perturbed complementarity conditions*

$$D_1\mathbf{z} = p\,\mathbf{e} \quad \text{and} \quad D_2\mathbf{w} = p\,\mathbf{e}. \tag{27}$$

Our primal–dual interior-point algorithm is based on a Newton–type method applied to three sets of equations: primal feasibility (x,q), dual feasibility (λ,η) and perturbed complementarity conditions, related to $(\mathbf{z},\mathbf{w})$. We denote by $\Phi := (x,q,\lambda,\eta,\mathbf{z},\mathbf{w})$ the solution of the optimization subproblem. Then, the *search direction* is given by $\triangle\Phi := (\triangle x, \triangle q, \triangle\lambda, \triangle\eta, \triangle\mathbf{z}, \triangle\mathbf{w})$. The update $\Phi \leftarrow \Phi + \triangle\Phi$ is determined by the increment $\triangle\Phi$ computed by using the Newton method for the following p-dependent system of equations:

$$K_p\ \triangle\ \Phi = -F_p(\Phi), \tag{28}$$

where (28) is often referred to as the *primal–dual* system and solved at each iteration with a decreasing positive parameter p. More precisely, (28) is equivalent to

$$\begin{pmatrix}
0 & \mathscr{L}_{xq} & \mathscr{L}_{x\lambda} & 0 & 0 & 0\\
\mathscr{L}_{qx} & \mathscr{L}_{qq} & \mathscr{L}_{q\lambda} & \mathscr{L}_{q\eta} & -\mathrm{I} & \mathrm{I}\\
\mathscr{L}_{\lambda x} & \mathscr{L}_{\lambda q} & 0 & 0 & 0 & 0\\
0 & \mathscr{L}_{\eta q} & 0 & 0 & 0 & 0\\
0 & Z & 0 & 0 & D_1 & 0\\
0 & -W & 0 & 0 & 0 & D_2
\end{pmatrix}
\begin{pmatrix}
\triangle x\\ \triangle q\\ \triangle\lambda\\ \triangle\eta\\ \triangle\mathbf{z}\\ \triangle\mathbf{w}
\end{pmatrix}
= -
\begin{pmatrix}
\nabla_x\mathscr{L}\\ \nabla_q\mathscr{L}\\ \nabla_\lambda\mathscr{L}\\ \nabla_\eta\mathscr{L}\\ \nabla_{\mathbf{z}}\mathscr{L}\\ \nabla_{\mathbf{w}}\mathscr{L}
\end{pmatrix}, \tag{29}$$

where I stands for the identity matrix, $Z = \mathrm{diag}(z_i)$ and $W = \mathrm{diag}(w_i)$ are diagonal matrices. The remaining nonzero entries of K_p are given by (24) and the following expressions:

$$\mathscr{L}_{\lambda x} = \mathscr{L}_{x\lambda}^{\mathrm{T}} = A(q), \quad \mathscr{L}_{\lambda q} = \mathscr{L}_{q\lambda}^{\mathrm{T}} = \partial_q(x^{\mathrm{T}}A(q)), \quad \mathscr{L}_{\eta q} = \mathscr{L}_{q\eta}^{\mathrm{T}} = \nabla^{\mathrm{T}}g(q). \tag{30}$$

Note that $\mathscr{L}_{\lambda x} = A(q)$ is the stiffness matrix of the electric potential equation, $\mathscr{L}_{qq}$ is a diagonal matrix and $\mathscr{L}_{\eta q} = \nabla^{\mathrm{T}}g(q)$ is just one row vector.

Now we eliminate the increments for $\mathbf{z}$ and $\mathbf{w}$ from the fifth and sixth rows of (29), namely,

$$\triangle\mathbf{z} = D_1^{-1}(-\nabla_{\mathbf{z}}\mathscr{L} - Z\triangle q),\ \ \triangle\mathbf{w} = D_2^{-1}(-\nabla_{\mathbf{w}}\mathscr{L} + W\triangle q). \tag{31}$$

Substituting (31) in the second row of (29), we get the following linear system for the increments of $\psi := (x, q, \lambda, \eta)$, denoted by $\triangle\psi := (\triangle x, \triangle q, \triangle\lambda, \triangle\eta)$:

$$\tilde{K}_p\,\triangle\psi = -\tilde{\tilde{\xi}}_p(\psi), \tag{32}$$

where $\tilde{K}_p$ is the matrix and $\tilde{\tilde{\xi}}_p(\psi)$ is the right-hand side of the following system:

$$\begin{pmatrix} 0 & \mathscr{L}_{xq} & \mathscr{L}_{x\lambda} & 0 \\ \mathscr{L}_{qx} & \tilde{\mathscr{L}}_{qq} & \mathscr{L}_{q\lambda} & \mathscr{L}_{q\eta} \\ \mathscr{L}_{\lambda x} & \mathscr{L}_{\lambda q} & 0 & 0 \\ 0 & \mathscr{L}_{\eta q} & 0 & 0 \end{pmatrix} \begin{pmatrix} \triangle x \\ \triangle q \\ \triangle\lambda \\ \triangle\eta \end{pmatrix} = - \begin{pmatrix} \nabla_x\mathscr{L} \\ \tilde{\nabla}_q\mathscr{L} \\ \nabla_\lambda\mathscr{L} \\ \nabla_\eta\mathscr{L} \end{pmatrix}. \tag{33}$$

The qq-entry of $\tilde{K}_p$ is now replaced by

$$\tilde{\mathscr{L}}_{qq} = \mathscr{L}_{qq} + D_1^{-1}\,Z + D_2^{-1}\,W,$$

and the modified entry for the right–hand side is

$$\tilde{\nabla}_q\mathscr{L} = \nabla_q\mathscr{L} + D_1^{-1}\,\nabla_{\mathbf{z}}\mathscr{L} - D_2^{-1}\,\nabla_{\mathbf{w}}\mathscr{L}.$$

The matrix K_p (from now on we omit the subscript p and denote the matrix by K) is typically indefinite. Similar indefinite systems of linear equations arise in the computation of saddle points when Stokes- and Navier–Stokes equations are solved. Iterative methods based, e.g., on the Uzawa algorithm for the solution of saddlepoint problems have been proposed in [2]. Direct methods for the solution can also be applied where direct *range space* and *null space* methods are distinguished. In [12], this distinction has been transferred to iterative methods.

First, let us consider the following *range space* formulation of K:

$$K = \begin{pmatrix} A & B^{\mathrm{T}} \\ B & D \end{pmatrix} = \begin{pmatrix} 0 & \mathscr{L}_{xq} & \mathscr{L}_{x\lambda} & 0 \\ \mathscr{L}_{qx} & \tilde{\mathscr{L}}_{qq} & \mathscr{L}_{q\lambda} & \mathscr{L}_{q\eta} \\ \mathscr{L}_{\lambda x} & \mathscr{L}_{\lambda q} & 0 & 0 \\ 0 & \mathscr{L}_{\eta q} & 0 & 0 \end{pmatrix}. \tag{34}$$

Here,

$$A = \begin{pmatrix} 0 & \mathscr{L}_{xq} \\ \mathscr{L}_{qx} & \tilde{\mathscr{L}}_{qq} \end{pmatrix} \quad \text{and } D = \begin{pmatrix} 0 & 0 \\ 0 & 0 \end{pmatrix},$$

so that in the Schur complement $S := D - BA^{-1}B^{\mathrm{T}}$ the first block A of K is taken as a pivot block and its definiteness plays a crucial role. In many practical applications, such as: (i) solving discrete saddlepoint problems arising in Stokes or Navier–Stokes equations; or (ii) linear programming problems, the block A is positive definite. For nonlinear convex problems (i.e., convex objective function, linear equality constraints and concave inequality constraints) the Hessian of the Lagrangian function

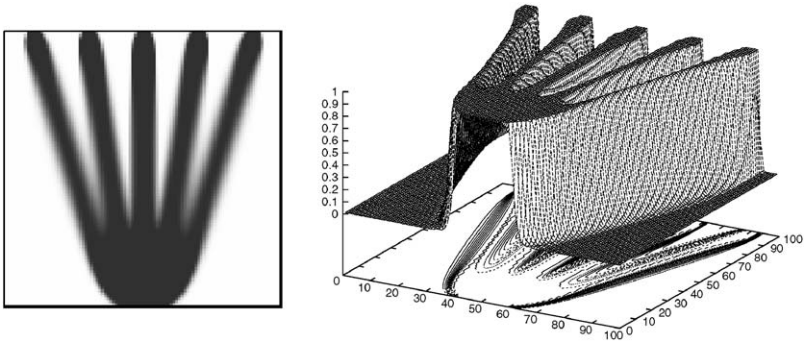

Fig. 4. Material distribution (100×100 mesh, 6 contacts).

is positive semidefinite. Preconditioned iterative solvers for the corresponding saddlepoint problems have been proposed, for example, in [10], and in the context of multigrid methods in [13].

We also consider the *null space* formulation of K:

$$K = \begin{pmatrix} A & B^{\mathrm{T}} \\ B & D \end{pmatrix} = \begin{pmatrix} 0 & \mathscr{L}_{x\lambda} & \mathscr{L}_{xq} & 0 \\ \mathscr{L}_{\lambda x} & 0 & \mathscr{L}_{\lambda q} & 0 \\ \mathscr{L}_{qx} & \mathscr{L}_{q\lambda} & \tilde{\mathscr{L}}_{qq} & \mathscr{L}_{q\eta} \\ 0 & 0 & \mathscr{L}_{\eta q} & 0 \end{pmatrix}, \tag{35}$$

where

$$A = \begin{pmatrix} 0 & \mathscr{L}_{x\lambda} \\ \mathscr{L}_{\lambda x} & 0 \end{pmatrix}$$

is now an indefinite, but nonsingular matrix. Moreover, we remind that $\mathscr{L}_{\lambda x} = A(q)$ is exactly the stiffness matrix corresponding to the electric potential Eq. (11). Hence, A^{-1} exists, and the Schur complement in this case $S = D - BA^{-1}B^{\mathrm{T}}$ is correctly defined. Furthermore, iterative solvers implementing A^{-1} are already available, which is a typical situation for optimization problems, where discretized differential equations form the bulk of the constraints. Therefore, the *null space* formulation turns out to be a more natural and attractive approach for solving the condensed primal–dual system, see, e.g., [5,9,15].

We use transforming *null space* iterations for our problem (33), as proposed in [9] in the context of multigrid methods. Transforming iterations have been introduced earlier as smoothers for multigrid methods in *range space* formulations by Wittum [13]. Here, these null space iterations are directly used as iterative solvers. Due to page limitations, we refer to [6] for more details. We conclude here by presenting an example of numerical results in Fig. 4.

Acknowledgements

This research has been supported by the German federal ministry for research and education (BMBF). The author thanks D. Logashenko, G. Wittum, R.H.W. Hoppe, and S. Petrova for joint

work on the practical applications mentioned in this paper. Furthermore he thanks the anonymous referees for invaluable comments and suggestions that helped to improve the paper.

References

[1] H. Ammari, A. Buffa, J.-C. Nédélec, A justification of eddy currents model for the maxwell equations, SIAM J. Appl. Math. 60 (5) (2000) 1805–1823.
[2] R. Bank, B. Welfert, H. Yserentant, A class of iterative methods for solving saddle point problems, Numer. Math. 56 (1990) 645–666.
[3] O. Biro, K. Preis, Various fem formulations for the calculation of transient 3d eddy currents in nonlinear media, IEEE Trans. Magnet. 31 (1995) 1307–1312.
[4] H.G. Bock, W. Egartner, W. Kappis, V. Schulz, Practical shape optimization for turbine and compressor blades, Optim. Eng. 3 (2002) 395–414.
[5] D. Gay, M. Overton, M. Wright, A primal–dual interior method for nonconvex nonlinear programming, in: Y. Yuan (Ed.), Advances in Nonlinear Programming, Kluwer, Dordrecht, 1998, pp. 31–56.
[6] R.H.W. Hoppe, S.I. Petrova, V.H. Schulz, A primal–dual Newton-type interior-point method for topology optimization, J. Optim. Theory Appl. 114 (3) (2002) 545–571.
[7] C. Lund, Ein Verfahren zur numerischen Simulation instationärer Strömungen mit nichtlinear-viskosen Fließeigenschaften, Fortschr.-Ber, VDI Reihe 7, Vol. 344, VDI Verlag, Düsseldorf, 1998.
[8] B. Maar, Nicht-Newtonsche Fluide. Mehrgitterverfahren für Bingham-Strömungen, Ph.D. Thesis, University of Stuttgart, 1998.
[9] B. Maar, V. Schulz, Interior point multigrid methods for topology optimization, Struct. Optim. 19 (2000) 214–224.
[10] T. Rusten, R. Winther, A preconditioned iterative method for saddlepoint problems, SIAM J. Matrix Anal. Appl. 13 (1992) 887–904.
[11] V.H. Schulz, Solving discretized optimization problems by partially reduced SQP methods, Comput. Visual. Sci. 1 (1998) 83–96.
[12] V.H. Schulz, G. Wittum, Multigrid optimization methods for stationary parameter identification problems in groundwater flow, in: W. Hackbusch, G. Wittum (Eds.), Multigrid Methods V, Lecture Notes in Computational Science and Engineering, Vol. 3, Springer, Berlin, 1998, pp. 276–288.
[13] G. Wittum, On the convergence of multigrid methods with transforming smoothers, Theory with application to the Navier–Stokes equations, Numer. Math. 57 (1989) 15–38.
[14] G. Wittum, V. Schulz, B. Maar, D. Logashenko, Numerical methods for parameter estimation in Bingham-fluids, in: W. Jäger, H.-J. Krebs (Eds.), Mathematics—Key Technology for the Future, Springer, Berlin, Heidelberg, 2003.
[15] M. Wright, Ill–conditioning and computational error in interior methods for nonlinear programming, SIAM J. Optim. 9 (1998) 84–111.